

Frictional properties of native and functionalized type I collagen thin films

Koo-Hyun Chung, Antony K. Chen, Christopher R. Anderton, Kiran Bhadriraju, Anne L. Plant et al.

Citation: *Appl. Phys. Lett.* **103**, 143703 (2013); doi: 10.1063/1.4824685

View online: <http://dx.doi.org/10.1063/1.4824685>

View Table of Contents: <http://apl.aip.org/resource/1/APPLAB/v103/i14>

Published by the [AIP Publishing LLC](#).

Additional information on *Appl. Phys. Lett.*

Journal Homepage: <http://apl.aip.org/>

Journal Information: http://apl.aip.org/about/about_the_journal

Top downloads: http://apl.aip.org/features/most_downloaded

Information for Authors: <http://apl.aip.org/authors>



Frictional properties of native and functionalized type I collagen thin films

Koo-Hyun Chung,¹ Antony K. Chen,^{2,3} Christopher R. Anderton,^{2,4} Kiran Bhadriraju,² Anne L. Plant,² Brian G. Bush,² Robert F. Cook,² and Frank W. DelRio^{2,a)}

¹*School of Mechanical Engineering, University of Ulsan, Ulsan 680-749, South Korea*

²*Material Measurement Laboratory, National Institute of Standards and Technology, Gaithersburg, Maryland 20899, USA*

³*Department of Biomedical Engineering, College of Engineering, Peking University, Beijing 100871, China*

⁴*Environmental Molecular Sciences Laboratory, Pacific Northwest National Laboratory, Richland, Washington 99354, USA*

(Received 22 July 2013; accepted 25 September 2013; published online 4 October 2013)

Frictional properties of native and fibronectin (FN)-functionalized type I collagen (COL) thin films were studied via atomic force microscopy. The COL lateral contact stiffness was dependent only on the hydration state, indicating that shear deformation was invariant with FN. In contrast, the COL coefficient of friction and shear strength varied with both functionalization and hydration state. The changes in shear strength were found to correlate well with changes in mean cell spread area on the same thin films, suggesting that shear strength is a better indicator of cell spreading than heretofore considerations of film, and thus extracellular matrix, stiffness alone. © 2013 AIP Publishing LLC. [<http://dx.doi.org/10.1063/1.4824685>]

The development, growth, and maintenance of normal tissue in the body are enabled by interactions between cells and the extracellular matrix (ECM).¹ These interactions are dictated not only by the composition of the ECM and the specific integrin receptors on the cell but also by the mechanical properties of the ECM.² As a result, it is necessary to study the mechanical properties of ECM constituents and correlate the properties to the cell response, as the resulting cell behavior-ECM properties relationships facilitate an improved understanding of cell migration, proliferation, and differentiation. In particular, the mechanical properties of collagen (COL) and fibronectin (FN) are of great interest, as they represent two of the most common proteins in the ECM. A number of groups have studied the folding and unfolding of single molecules and fibrils of COL and FN using atomic force microscopy (AFM),³⁻⁷ and in doing so, gained quantitative insight into molecular and sub-molecular properties (e.g., Young's modulus, Poisson's ratio, contour and persistence lengths). However, there are obvious difficulties related to investigating cell behavior on single molecules or fibrils and thus with establishing the aforementioned behavior-properties relationships. As a result, recent work has focused on the development of robust and reproducible thin films of COL fibrils^{8,9} to more readily examine the effects of ECM composition and mechanics on cell behavior.¹⁰⁻¹³ More specifically, these model ECMs were used to correlate the normal contact stiffness, often interpreted in terms of Young's modulus, to cell spreading on COL films subjected to dehydration,^{10,11} low and high vacuum,¹² and FN-functionalization.¹³ In this Letter, we study the *shear* contact properties of native and FN-functionalized type I COL films with AFM and correlate the properties with mean cell spread areas on the same films, as cells are known to generate *lateral* movement of the ECM.¹⁰ A key feature of our approach is the separate determination of the lateral

contact stiffness of the films, characterizing the resistance of the films to shear deformation, and the *shear strength* of the film-AFM probe interface, characterizing the resistance of the interface to failure. Previous studies have focused on the former, the reversible deformation of the contact; here, we extend these studies to consider the irreversible failure of the contact, associated with adhesive instability and fracture.

Type I COL thin films with and without FN were deposited as previously described.^{9,12,13} Briefly, acidified COL monomer was diluted to 300 $\mu\text{g}/\text{ml}$ using phosphate buffered saline (PBS) and further neutralized with sodium hydroxide. The resulting solution was incubated on 50 mm bacterial-grade polystyrene dishes overnight at 37 °C to facilitate COL polymerization and fibril assembly on the surface. Excess COL solution was aspirated from the sample, and the remaining surface-adhered COL was rinsed with PBS and >18.2 M Ω cm deionized (DI) water. COL films were then exposed to a stream (30 s to 60 s) of filtered N₂ to remove excess DI water from the fibril surface, which resulted in a COL film with large (\approx 200 nm in diameter) fibrils on top of a bed of smaller (\approx 75 nm in diameter) fibrils.^{8,9} At this time, the samples were divided into two groups: the "untreated" COL films were stored in PBS at 4 °C and the "dehydrated" COL films were dried for 24 h in a laminar flow hood and then stored in PBS at 4 °C (the dehydration *is not* physiologically appropriate, but does facilitate changes to mechanical properties without drastically altering integrin recognition or surface topography, thereby enabling cell behavior-mechanical property relationships that *are* physiologically relevant). Samples from each group were also incubated in 3 ml of a 25 $\mu\text{g}/\text{ml}$ PBS-based FN solution for 24 h prior to storage in PBS at 4 °C, thus forming both untreated COL/FN and dehydrated COL/FN composite films. FN binds to COL¹⁴ via a site about 30 kDa from the amino terminus on the FN¹⁵ and residues 757 to 791 on the COL.^{16,17} Intermittent-contact mode AFM images of some of the COL films are shown in Fig. 1, both in PBS solution and in air at 25 °C. In Figs. 1(a) and 1(b), the images of the untreated and dehydrated COL in PBS highlight the large

^{a)} Author to whom correspondence should be addressed. Electronic mail: frank.delrio@nist.gov

fibrils and the reduction in film thickness from the dehydration procedure (FN has a negligible impact on film topography, as shown previously with AFM¹³). In Figs. 1(c) and 1(d), the images in air reveal the smaller fibril bed and the expected periodic banding patterns in the large fibrils.^{5-7,11}

Lateral force measurements on the films were also carried out in an AFM in PBS solution at 25 °C using both colloidal sphere and sharp probe tips. In the colloidal probe experiments, a gold sphere ($\approx 25 \mu\text{m}$ in diameter) was attached to the end of a rectangular AFM cantilever using a two-part, room temperature epoxy. The torsional spring constant k_{lev} of the colloidal probe was obtained via the calibrated reference cantilever method¹⁸ in air; k_{lev} at the bottom of the sphere was found to be $0.98 \pm 0.07 \text{ N/m}$ using a separate reference cantilever with a normal spring constant of $1.84 \pm 0.09 \text{ N/m}$ (unless stated otherwise, experimental uncertainties are one standard deviation of the sample population mean). The lateral optical lever sensitivity S_{lev} of the colloidal probe was then acquired by laterally pressing the equator of the sphere against a rigid surface in PBS solution; S_{lev} at the bottom of the sphere was $0.019 \pm 0.001 \text{ V/nm}$. In the sharp probe experiments, cantilevers with integrated gold-coated probe tips ($\approx 60 \text{ nm}$ in diameter) were used. k_{lev} values for the sharp probes were determined via torsional beam theory.^{19,20} The geometric properties (length, thickness, width, and tip height) for this approach were found with confocal microscopy and scanning electron microscopy, whereas the mechanical properties (Young's modulus and shear modulus) were found from the measured normal spring constants²¹ coupled with flexural beam theory; the latter analysis resulted in an average Young's modulus of 146 GPa and a shear modulus of 56 GPa (assuming a Poisson's ratio of 0.30), in good agreement with results for silicon nitride cantilevers.²² k_{lev} ranged from 0.9 N/m to 1.1 N/m. The multiple location pivot method²³ was then used to obtain the lateral force sensitivities T_{lev} for the sharp tips in PBS solution; T_{lev} varied from $0.14 \pm 0.02 \text{ V/nN}$ to $0.16 \pm 0.02 \text{ V/nN}$ (uncertainties represent the standard error in the method fit).

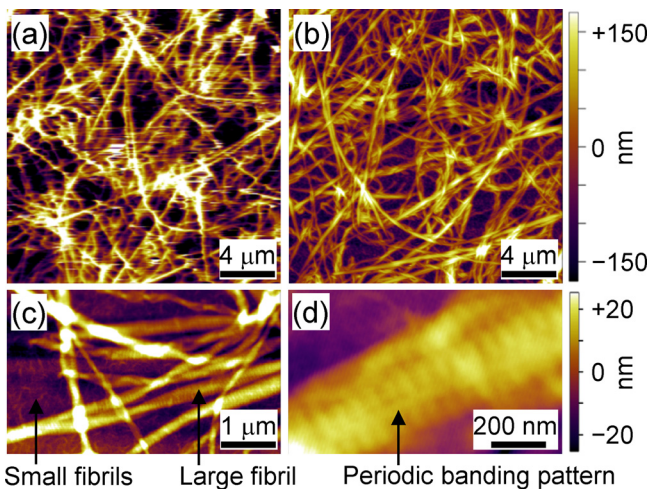


FIG. 1. Intermittent-contact mode AFM images of the COL films in (a) and (b) PBS solution and (c) and (d) air at 25 °C. In PBS solution, the images of the (a) untreated and (b) dehydrated COL films highlight the large fibrils and the reduction in film thickness from dehydration. In air, the images reveal the (c) small fibril bed and the (d) periodic banding patterns in the large fibrils.

Figure 2 shows the lateral force measurements on the COL films with a gold colloidal probe; this probe type allows for measurement of mechanical properties over areas similar to cell spread areas, which translates to contact with the small fibril bed and several large fibrils as shown schematically in Fig. 2(a). Friction loops in the trace (upper, probe moving left) and retrace (lower, probe moving right) directions for the untreated and dehydrated COL films with and without FN at a normal force $F_n = 0.27 \text{ nN}$ are shown in Fig. 2(b). In all four loops, smooth sliding is observed over a majority of the trace (i.e., the lateral force F_f is constant over the lateral displacement x). However, there are several instances of stick-slip behavior, particularly for the untreated COL films, likely as the tip interacts with (and detaches from) the large fibrils on the COL surface. Several stick-slip events exhibit multiple instabilities, indicative of multiple fibrils attached to the probe tip in parallel.²⁴ Average values for F_f as a function of F_n are shown in Fig. 2(c). Overall, F_f varied almost linearly with F_n for all films (for clarity, only

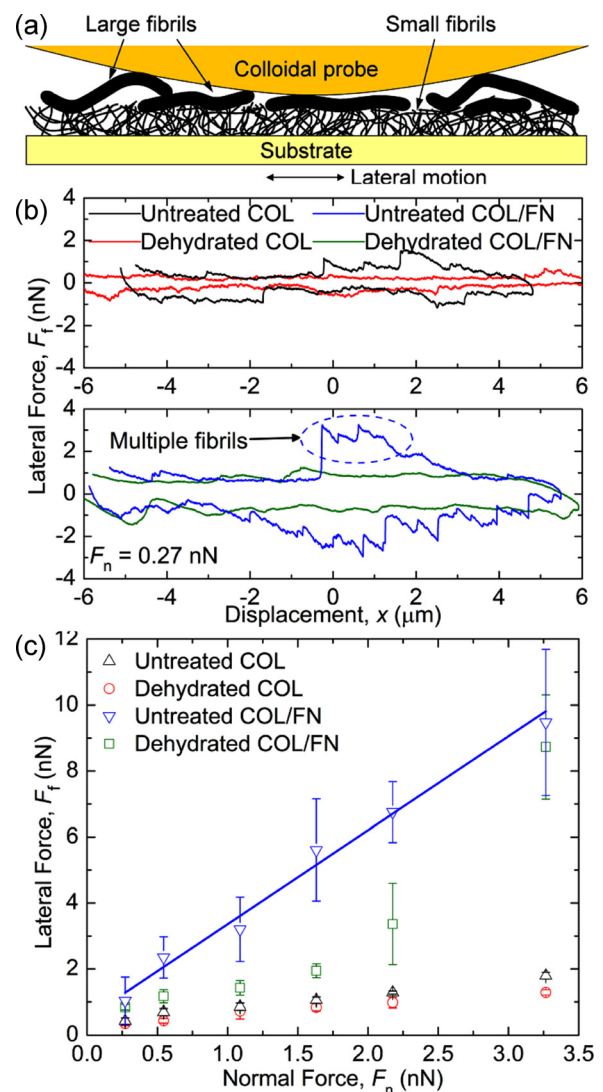


FIG. 2. (a) Schematic diagram of a colloidal probe in contact with a COL film. F_f as a function of (b) x and (c) F_n for the untreated and dehydrated COL films with and without FN. In (b), smooth sliding and stick-slip behavior with multiple instabilities are observed. In (c), F_f varies linearly with F_n for all films; the solid line represents a linear fit to the untreated COL/FN data, with μ as the slope.

TABLE I. The extracted values for μ , k_{fib} , and τ for the untreated and dehydrated COL films with and without FN. A_{cs} values taken from Ref. 13. Uncertainty values represent the standard error in the fit or one standard deviation of the mean.

| | Untreated COL | Untreated COL/FN | Dehydrated COL | Dehydrated COL/FN |
|--|------------------|------------------|------------------|-------------------|
| μ^{a} | 0.43 ± 0.02 | 2.85 ± 0.19 | 0.32 ± 0.01 | 0.94 ± 0.25 |
| k_{fib} (N/m) ^b | 0.03 ± 0.01 | 0.03 ± 0.01 | 0.05 ± 0.01 | 0.05 ± 0.01 |
| τ (kPa) ^a | 145.6 ± 12.5 | 303.1 ± 43.0 | 327.1 ± 13.2 | 871.5 ± 100.4 |
| A_{cs} (μm^2) ^b | 2919 ± 345 | 4071 ± 323 | 5458 ± 87 | 6883 ± 326 |

^aStandard error in the fit.

^bStandard deviation of the mean.

one fit line is shown). Two potential reasons for the linearity include: (1) plastic deformation in the films²⁵ or (2) elastic deformation between the AFM probe tip and multiple fibrils.²⁶ In (1) and (2), F_f can be represented by $F_f = \mu F_n$, where the complexity of the coefficient of friction μ can vary from something as simple as the ratio of shear strength to yield strength²⁵ to something dependent on many geometric and material properties.²⁶ Despite the difficulties in interpreting μ , the values show a clear dependency on both the hydration state and the presence of FN, as shown in Table I.

The dehydrated COL films exhibited a slightly smaller average F_f than the untreated COL films, particularly at larger F_n , as shown in Fig. 2(c). The decrease in F_f is likely due to a two-fold change in the COL films as a result of the dehydration. First, there is a considerable increase in the Young's modulus and decrease in the thickness of the small and large fibril beds,^{10,11} both of which lead to smaller contact areas A_c and therefore smaller F_f . Second, the dehydration process greatly reduces the mobility of the large fibrils; in previous work,²⁷ untreated COL fibrils were displaced with F_n of 5 nN, whereas dehydrated COL fibrils could not be displaced with the maximum F_n available with the AFM instrument and tip, indicating that the dehydrated fibrils are far more likely to exhibit smooth sliding and the associated smaller F_f values as shown in Fig. 2(b). The addition of FN to the COL was found to have a much greater effect on the lateral force; F_f increased by $\approx 4\times$ and $\approx 3\times$ for the untreated and dehydrated COL films, respectively. The dramatic increases associated with FN are not due to changes in the topography or Young's modulus, as the size of the fibrils is invariant and the Young's modulus increases,¹³ the latter leading to a decrease, not an increase, in A_c and F_f . Therefore, the changes in F_f cannot be solely due to the factors above.

Figure 3 shows the lateral force measurements on the COL films with a sharp probe tip. As shown schematically in Fig. 3(a), the sharp probe is different than its colloidal counterpart in that it interlocks and manipulates individual fibrils instead of resting on top of them. This is clear from the friction data in Fig. 3(b), as the number of stick-slip events with a single instability increased. These events are separated by 100s of nm, which represents distances much larger than those reported by Gutschmann *et al.*²⁸ for individual COL molecules (namely, 78 nm for the major binding distance and 22 nm for the minor binding distance). Thus, the events are likely due to interactions between the probe tip and entire COL fibrils, as opposed to interactions between the probe and individual COL molecules. The total lateral stiffness k_{tot} of each fibril is the slope of the load-displacement behavior

for each stick-slip event. The fibril contact stiffness k_{fib} can be calculated from k_{lev} and k_{tot} by $k_{\text{fib}} = (1/k_{\text{tot}} - 1/k_{\text{lev}})^{-1}$. However, because $k_{\text{lev}} \gg k_{\text{tot}}$, $k_{\text{fib}} \approx k_{\text{tot}}$. Moreover, F_f varied sublinearly with F_n for all films as shown in Fig. 3(c), in agreement with contact mechanics models based on adhesive contact in the presence of interfacial forces. As a result, F_f is related to the interfacial shear strength τ by $F_f = \tau A_c$, with the relationship between A_c and F_n defined by an appropriate

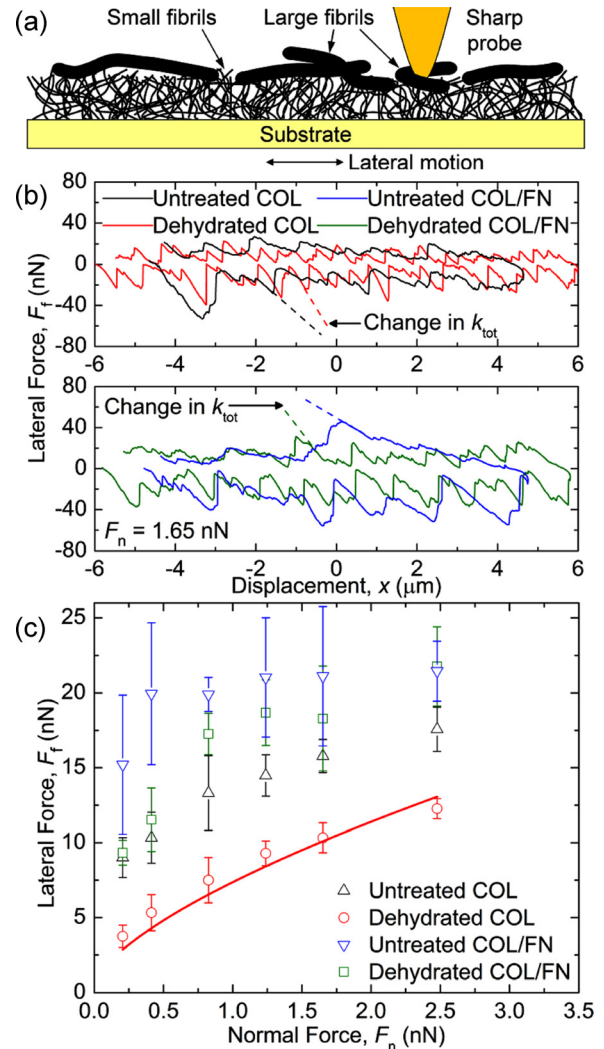


FIG. 3. (a) Schematic diagram of a sharp probe in contact with a COL film. F_f as a function of (b) x and (c) F_n for the untreated and dehydrated COL films with and without FN. In (b), there are a number of stick-slip events with a single instability, the slope of which are k_{tot} . In (c), F_f varies sublinearly with F_n for all films; the solid line represents a fit to the dehydrated COL data using the JKR model, with τ as the fitting parameter.

contact model (here, the Johnson–Kendall–Roberts (JKR) model²⁹). The lone fitting parameter is τ , as the Young's moduli and works of adhesion are known from earlier work,¹³ and the probe radius and Poisson's ratio are taken from nominal or assumed values.³⁰

As shown in Fig. 3(b), the friction traces for the dehydrated COL films were much different than those for the untreated COL films. In particular, k_{tot} (and hence k_{fib}) changed from $0.03 \text{ N/m} \pm 0.01 \text{ N/m}$ for the untreated COL to $0.05 \text{ N/m} \pm 0.01 \text{ N/m}$ for the dehydrated COL. Therefore, the dehydrated COL fibrils are almost twice as stiff as the untreated COL fibrils, as shown in Table I. McDaniel *et al.*¹⁰ reported k_{fib} for similar untreated and dehydrated COL films up to an order of magnitude less than those here. However, in that study, k_{fib} was ascertained using normal force spectroscopy, signifying that a stiff cylindrical beam on a compliant elastic foundation may be more compliant in the normal direction than in the lateral direction. Despite the differences, it is clear that the dehydrated fibrils are stiffer than the untreated fibrils due to an increase in the interfibril attractive forces.³¹ Specifically, the absence of water results in additional and shorter intramolecular hydrogen bonds, which bring about a stiffer molecular structure.^{10,32,33} As shown in Fig. 3(c), both data sets are well-described by the JKR model (for clarity, only one fit line is shown). From the JKR fits, τ was found to increase from $145.6 \text{ kPa} \pm 12.5 \text{ kPa}$ for the untreated COL to $327.1 \text{ kPa} \pm 13.2 \text{ kPa}$ for the dehydrated COL, providing further evidence that dehydration results in films more resistant to shear forces.²⁷ The addition of FN to the COL did not have an impact on k_{fib} , but did result in a $\approx 2\times$ and $\approx 3\times$ increase in τ for the untreated COL and dehydrated COL, respectively. The dehydrated COL is more disposed to FN-based changes to τ than the untreated COL; variations in the conformational state of FN^{34–36} from changes in the surface and bulk properties of the COL¹² may explain the differences in the increase to τ . Despite the differences, the increases from FN are in good agreement with the increases for other functionalized COL, which range between $1.2\times$ and $12\times$.^{27,37–39} Additionally, the increases in τ from FN elucidate the increases in F_f observed with the colloidal probe in Fig. 2.

Chen *et al.*¹³ investigated fluorescence microscopy images of A10 rat aortic vascular smooth muscle cells (vSMCs) labeled with Texas Red-C2-Maleimide after 24 h incubation on the same series of COL films. The mean vSMC spread area A_{cs} increased in the following order: (a) untreated COL, (b) untreated COL/FN, (c) dehydrated COL, and (d) dehydrated COL/FN. Interestingly, τ increases as A_{cs} increases, as shown in Table I. The significance of shear properties on cell behavior was qualitatively recognized by McDaniel *et al.*¹⁰ via time-lapsed images of vSMCs on COL films; the images provided visual evidence that cells initiate lateral movement of individual COL fibrils on the order of $1 \mu\text{m}$ to $5 \mu\text{m}$. Spurlin *et al.*²⁷ also acknowledged the importance of shear properties on cell behavior via lateral movement experiments on untreated, dehydrated, and transglutaminase-functionalized COL. The observations, although informative, could not distinguish unambiguously which of the mechanical properties of the film in shear was determining cell response. Heretofore, film normal stiffness,

often interpreted in terms of Young's modulus but linearly related to film lateral stiffness, has been regarded as the primary factor in determining cell behavior; the lateral motion induced in the COL fibrils comprising the film implies that resistance to deformation must play a role in cell motion.^{10–13} However, without quantitative F_f measurements, the role of resistance to adhesive shear failure between the cell and the fibrils could not be assessed. Such failure occurs when the rate of mechanical energy decrease on cell-fibril deformation exceeds the rate of cell-fibril surface energy increase at the contact.²⁹ Here, this instability was characterized by the frictional shear strength τ : The much stronger correlation between τ and A_{cs} than between k_{fib} and A_{cs} suggests that changes in cell spreading are determined by considerations of both deformation and adhesion rather than deformation alone.

In summary, the frictional properties of untreated and dehydrated COL with and without FN were investigated via AFM using colloidal sphere and sharp probe tips. In both cases, the F_f curves revealed stick-slip events from the tip interacting with COL fibrils; the colloidal probe tip interacted with multiple fibrils in parallel, while the sharp tip manipulated individual fibrils. The resulting k_{fib} values were dependent only on the hydration state, indicating that FN does not have an appreciable impact on the bending properties of the COL fibrils. In contrast, μ and τ were dependent on both the hydration state and the FN, signifying that the shear properties are changed by functionalization and dehydration. The changes in τ were found to correlate well with the changes in A_{cs} , suggesting that τ is a much better indicator of cell behavior on COL films, and thus the ECM, than considerations of stiffness alone. Future work on other ECM proteins will investigate this possibility, and in doing so, enable similar behavior-property relationships to be established.

K.H.C. acknowledges financial support from the National Research Foundation of Korea (NRF) Grant funded by the Korean Government (MSIP) (No. 2011-0014367).

¹K. M. Yamada, *Annu. Rev. Biochem.* **52**, 761 (1983).

²A. L. Plant, K. Bhadriraju, T. A. Spurlin, and J. T. Elliott, *Biochim. Biophys. Acta* **1793**, 893 (2009).

³Y. Oberdörfer, H. Fuchs, and A. Janshoff, *Langmuir* **16**, 9955 (2000).

⁴L. Bozec and M. Horton, *Biophys. J.* **88**, 4223 (2005).

⁵A. J. Heim, W. G. Matthews, and T. J. Koob, *Appl. Phys. Lett.* **89**, 181902 (2006).

⁶C. A. Grant, D. J. Brockwell, S. E. Radford, and N. H. Thomson, *Appl. Phys. Lett.* **92**, 233902 (2008).

⁷M. P. E. Wenger and P. Mesquida, *Appl. Phys. Lett.* **98**, 163707 (2011).

⁸J. T. Elliot, A. Tona, J. T. Woodward, P. L. Jones, and A. L. Plant, *Langmuir* **19**, 1506 (2003).

⁹J. T. Elliot, M. Halter, A. L. Plant, J. T. Woodward, K. J. Langenbach, and A. Tona, *BioInterphases* **3**, 19 (2008).

¹⁰D. P. McDaniel, G. A. Shaw, J. T. Elliott, K. Bhadriraju, C. Meuse, K.-H. Chung, and A. L. Plant, *Biophys. J.* **92**, 1759 (2007).

¹¹K.-H. Chung, K. Bhadriraju, T. A. Spurlin, R. F. Cook, and A. L. Plant, *Langmuir* **26**, 3629 (2010).

¹²C. R. Anderton, F. W. DelRio, K. Bhadriraju, and A. L. Plant, *BioInterphases* **8**, 1 (2013).

¹³A. K. Chen, F. W. DelRio, A. W. Peterson, K.-H. Chung, K. Bhadriraju, and A. L. Plant, *Biotechnol. Bioeng.* **110**, 2731 (2013).

¹⁴R. J. Klebe, *Nature* **250**, 248 (1974).

¹⁵G. Balian, E. M. Click, and P. Bornstein, *J. Biol. Chem.* **255**, 3234 (1980).

¹⁶W. Dessau, B. C. Adelman, R. Timpl, and G. R. Martin, *Biochem. J.* **169**, 55 (1978).

- ¹⁷H. K. Kleinman, E. B. McGoodwin, G. R. Martin, R. J. Klebe, P. P. Fietzek, and D. E. Woolley, *J. Biol. Chem.* **253**, 5642 (1978).
- ¹⁸K.-H. Chung, J. R. Pratt, and M. G. Reitsma, *Langmuir* **26**, 1386 (2010).
- ¹⁹E. Liu, B. Blanpain, and J. P. Celis, *Wear* **192**, 141 (1996).
- ²⁰R. J. Cannara, M. Eglin, and R. W. Carpick, *Rev. Sci. Instrum.* **77**, 053701 (2006).
- ²¹J. L. Hutter and J. Bechhoefer, *Rev. Sci. Instrum.* **64**, 1868 (1993).
- ²²M. A. Lantz, S. J. O'Shea, A. C. F. Hoole, and M. E. Welland, *Appl. Phys. Lett.* **70**, 970 (1997).
- ²³K.-H. Chung and M. G. Reitsma, *Rev. Sci. Instrum.* **81**, 026104 (2010).
- ²⁴G. Stan, F. W. DelRio, R. I. MacCuspie, and R. F. Cook, *J. Phys. Chem. B* **116**, 3138 (2012).
- ²⁵F. P. Bowden and D. Tabor, *The Friction and Lubrication of Solids* (Oxford University Press, New York, 2001).
- ²⁶J. A. Greenwood and J. B. P. Williamson, *Proc. R. Soc. London, Ser. A* **295**, 300 (1966).
- ²⁷T. A. Spurlin, K. Bhadriraju, K.-H. Chung, A. Tona, and A. L. Plant, *Biomaterials* **30**, 5486 (2009).
- ²⁸T. Gutsmann, G. E. Fantner, J. H. Kindt, M. Venturoni, S. Danielsen, and P. K. Hansma, *Biophys. J.* **86**, 3186 (2004).
- ²⁹K. L. Johnson, K. Kendall, and A. D. Roberts, *Proc. R. Soc. London, Ser. A* **324**, 301 (1971).
- ³⁰V. H. Barocas, A. G. Moon, and R. T. Tranquillo, *J. Biomed. Eng.* **117**, 161 (1995).
- ³¹J. Rosenblatt, B. Devereux, and D. G. Wallace, *Biomaterials* **15**, 985 (1994).
- ³²I. G. Mogilner, G. Ruderman, and J. R. Grigera, *J. Mol. Graphics Modell.* **21**, 209 (2002).
- ³³A. George and A. Veis, *Biochemistry* **30**, 2372 (1991).
- ³⁴E. C. Williams, P. A. Janmey, J. D. Ferry, and D. F. Mosher, *J. Biol. Chem.* **257**, 14973 (1982).
- ³⁵A. J. Garcia, M. D. Vega, and D. Boettiger, *Mol. Biol. Cell* **10**, 785 (1999).
- ³⁶B. G. Keselowsky, D. M. Collard, and A. J. Garcia, *J. Biomed. Mater. Res. Part A* **66**, 247 (2003).
- ³⁷L. Yang, K. O. van der Werf, C. F. C. Fitie, M. L. Bennink, P. J. Dijkstra, and J. Feijen, *Biophys. J.* **94**, 2204 (2008).
- ³⁸W. T. Brinkman, K. Nagapudi, B. S. Thomas, and E. L. Chaikof, *Biomacromolecules* **4**, 890 (2003).
- ³⁹D. M. O. Halloran, R. J. Collighan, M. Griffin, and A. S. Pandit, *Tissue Eng.* **12**, 1467 (2006).